Available online at www.sciencedirect.com
ScienceDirect
Advances in Space Research 39 (2007) 1439–1444
ADVANCES IN SPACE RESEARCH (a COSPAR publication)
www.elsevier.com/locate/asr

An analysis of solar radio burst events on December 1, 2004

Jing Huang [a,b,*], Yihua Yan [a], Yuying Liu [a]

[a] National Astronomical Observatories, Chinese Academy of Sciences, Datun Road A20, Chaoyang district, Beijing 100012, China
[b] Graduate University, Chinese Academy of Sciences, Yuquan Road 19A, Beijing 100049, China

Received 30 October 2006; received in revised form 22 March 2007; accepted 22 March 2007

Abstract

We present the analysis of the radio observations of December 1, 2004 from 07:00 UT to 07:40 UT in the 1.100–1.340 GHz band by Solar Broadband Radio Dynamic Spectrometer (SBRS) in Huairou Station. There are three groups of radio fine structures during the impulsive phase of this flare denoted by N1, Z2, and Z3. N1 has several emission lines with mixed fast and slow frequency drift rate which may reflect the conditions of flare loop and fast flows out from reconnection site; Z2 and Z3 are zebra patterns. The radio observations combined with hard X-ray and other observations show that the fine structures are connected with energetic particles. The information about magnetic field and energetic particle during the burst are also estimated based on our model.

Keywords: Solar radio burst; Zebra pattern; Coronal loop

1. Introduction

Solar radio emission from flares play an important role in understanding energy release, plasma heating, particle acceleration and particle transport in magnetized plasmas. Especially, the fine structures may help us to look into the dynamical process during the burst of flares (Bastian et al., 1998; Aschwanden, 2004). Radio observations combined with hard X-ray (HXR) observations can help us to analyze the release of flare energy and acceleration of energetic particles during the flare.

Solar radio fine structures such as zebra pattern structures and fiber bursts superimposed on microwave bursts were classified and studied more than 20 years ago (Kruger, 1979; Slottje, 1981). The generally accepted mechanism for the fiber burst is the interactions between electrostatic plasma waves and whistlers, both excited by the same population of fast electrons, which have a loss-cone velocity distribution. Most models of zebra pattern include the emission of electrostatic plasma waves at double plasma-resonance (DPR) frequency (Kuijpers, 1975; Zhelezniakov and Zlotnik, 1975):

$$\omega_{\mathrm{UH}} = (\omega_{\mathrm{pe}}^2 + \omega_{\mathrm{Be}}^2)^{1/2} = s\omega_{\mathrm{Be}} \tag{1}$$

where ω_{UH} is the upper-hybrid frequency, ω_{pe} is the electron plasma frequency, ω_{Be} is the electron cyclotron frequency, and s is the harmonic number. But, the improvement in time and the frequency resolutions reveal plenty of new features that can not be easily explained by the DPR model. To explain these new features, Chernov (1976, 1996) and Chernov et al. (2005) developed the DPR model to whistler model. Other models are also available (e.g., LaBelle et al., 2003; Ledenev et al., 2006).

Using the extremely high resolution mode (4 MHz in 1.25 ms) in the 1.100–1.340 GHz ranges, a large amount of microwave bursts and fine structures were obtained by Solar Broadband Radio Dynamic Spectrometer (SBRS) in Huairou Station (Fu et al., 2004; Ji et al., 2005). The flare on December 1, 2004 of active region 10708 was also recorded by SBRS in the 1.100–1.340 GHz band (Liu et al., 2006). Three groups of fine structures (FS) have been

* Corresponding author. Address: National Astronomical Observatories, Chinese Academy of Sciences, Datun Road A20, Chaoyang district, Beijing 100012, China.
E-mail address: huangjing04@bao.ac.cn (J. Huang).

0273-1177/$30
doi:10.1016/j.asr.2007.03.061

found. When analyzing these fine structures, a new kind of mixed fast-and-slow drifting stripes is found before two groups of zebra pattern or fiber structures, which may correspond to the fast downward flow and slow upward flare loop in the cusp area. Here we present the analysis of the three fine structures. With the whistler model presented by Chernov et al. (2001) and DPR theory we can estimate the magnetic field and the density of plasma inside the flare loop. We then compare the result with our dipole model of AR 10708 and to estimate the positions where the two zebra structures may occur in our model of the coronal loop, so that in the process of the radio bursts, the change of magnetic field and the acceleration of energetic electrons during the flare could be understood.

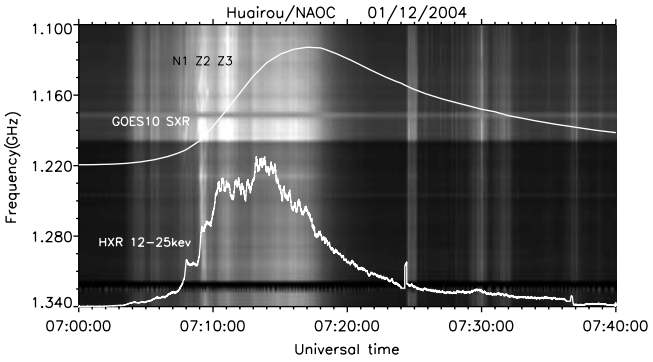

Fig. 2. The radio dynamic spectrum of the December 1, 2004 flare from 07:00:00 UT to 07:40:00 UT in 1.100–1.340 GHz band. The time profile of HXR flux at 12–25 keV band from HESSI and SXR flux from GOES10 are over plotted. Three fine structures during the burst are denoted by N1, Z2, and Z3.

2. New observational data and analysis

2.1. Observational data

A flare, occurred on December 1, 2004 in NOAA Active Region 10708, located close to the center of solar disk (N9E20), was recorded by GOES and RHESSI (Lin et al., 2002). The begin time, peak time and end time of $H\alpha$ flare occurred in AR 10708 are 07:06 UT, 07:15 UT, and 08:21 UT as provided by SGD. Fig. 1 shows the MDI magnetogram (Scherrer et al., 1995) and EIT image (Delaboudiniere et al., 1995) of AR 10708 on December 1, 2004. From the EIT picture, the flare has several loops brightening during the burst. During the flare, radio bursts were also observed by Huairou station. Fig. 2 shows the total radio burst from 07:00:00 UT to 07:40:00 UT in the 1.100–1.340 GHz band with 4 MHz spectral resolution but with 0.2 s cadence, over-plotted with the time profiles of GOES soft X-ray (SXR) flux and RHESSI HXR flux at 12–25 keV band. During the impulsive phase of this flare (from 07:10 UT to 07:15 UT), three groups of fine structure appeared, which are denoted by N1, Z2, and Z3, respectively. The detailed fine structure patterns are shown in Fig. 3. Fig. 3(a) shows the spectrum of radio emission at 1.100–1.340 GHz from 07:07:00 UT to 07:12:00 UT, with HXR time profiles at both 12–25 keV and 25–50 keV bands observed by RHESSI over-plotted. During the impulsive phase of this flare, the HXR emissions at both bands were increasing quickly and the HXR flux seems to maintain at a plateau while each radio fine structure occurred. The peak time of radio flux at 1.200 GHz of each events are: 07:08:00 UT, 07:09:05 UT, 07:11:00 UT.

The detailed spectra of N1, Z2, and Z3 are shown in Figs. 3(b–d). The HXR time profiles at 12–25 keV band were over-laid on the dynamic spectra. Although the time profiles of radio flux is a bit different from the time profiles of HXR flux, both of them have obvious oscillations during N1, Z2, and Z3. During each event, the HXR flux seemed to maintain at a plateau with lots of oscillations, especially for Z2 and Z3 bursts. Hence, the radio fine structures are connected with energetic electrons directly. During each radio fine structure, the energetic particles are influenced by the plasma inside the flare loops and the

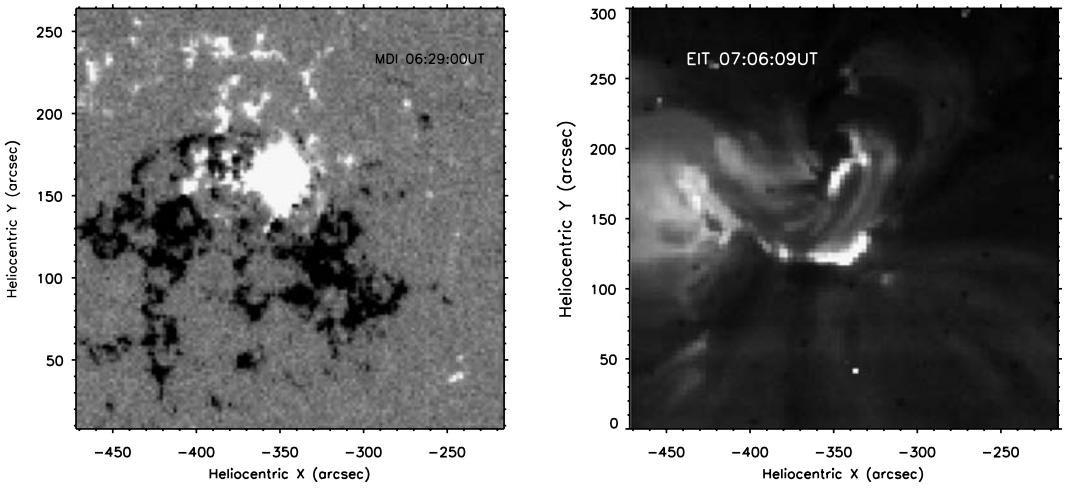

Fig. 1. Left panel: MDI magnetogram of AR 10708 at 06:29:00 UT on December 1, 2004 in AR 10708. Right panel: The EIT data from SOHO at 07:06:09 UT on December 1, 2004 in AR 10708 at 284 Å.

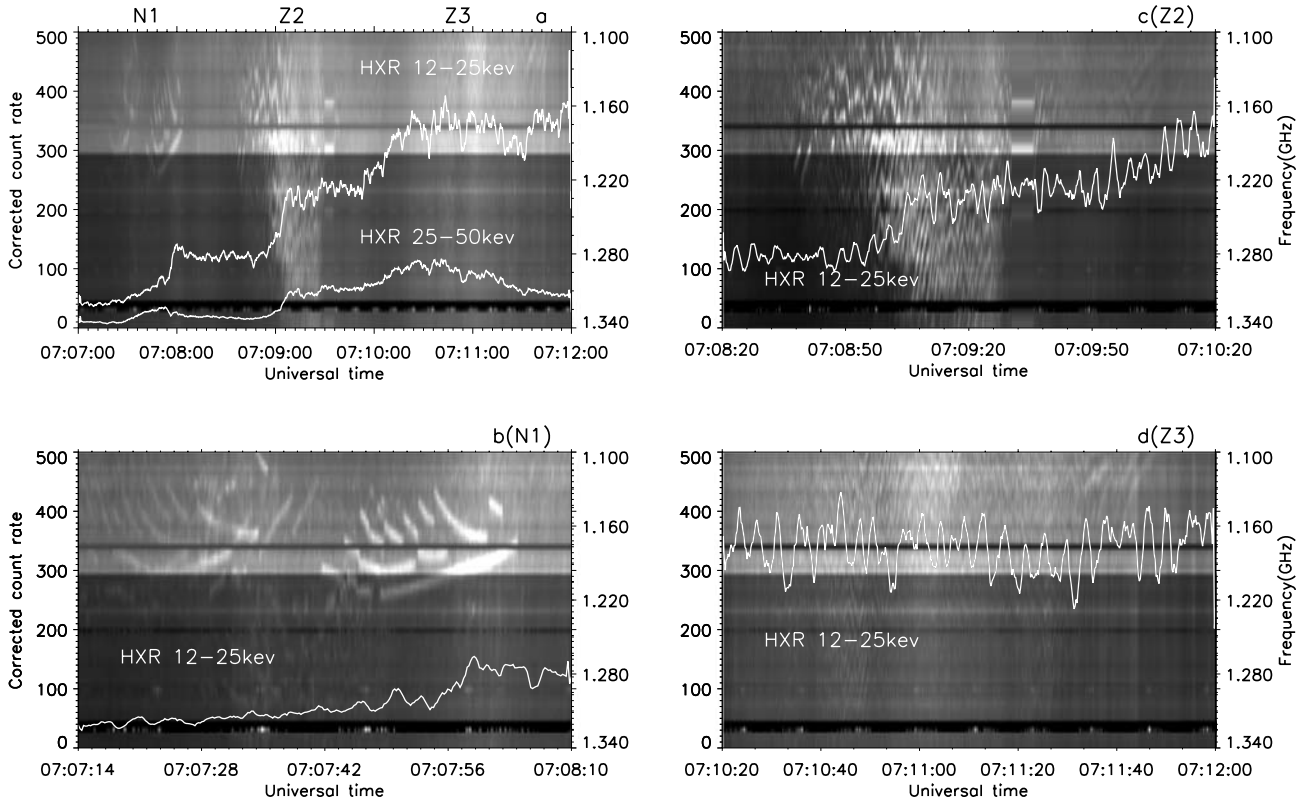

Fig. 3. (a) The spectra of the three fine structures from 07:07:00 UT to 07:12:00 UT in 1.100–1.340 GHz band with HXR time profiles plotted over. (b) N1 fine structure in detail with 12–25 keV HXR time profile plotted over. (c) and (d) Z2 and Z3 fine structures in detail. The 12–25 keV HXR time profiles plotted over them.

HXR flux did not increase continuously, but maintained as a plateau with three different levels increased progressively. N1 is a new fine structure with mixed fast-and-slow frequency drift rate which we will analyze in Section 2.2. Obviously, Z2 and Z3 are zebra pattern structures, but, the frequency differences between two neighboring zebra lines are different from each other. Fine structures are not found at high frequency bands i.e. 2.600–3.800 GHz and 5.200–7.600 GHz by Huairou Radio Spectrometers (Fu et al., 2004).

2.2. Analysis of N1

N1 has several emission stripes with different fast and slow drifting rates which is obviously different from the classical zebra patterns. The left part and right part of N1 have the similar structure. The parameters of the right part of N1 (from 07:07:30 UT to 07:09:00 UT) are shown in Table 1. The mean fast frequency drift of stripes at high altitude (low frequency) is about 11.9 MHz/s and the slow frequency drift rate of the stripes at lower altitude (high frequency) is about −3.8 MHz/s. The time interval of stripes are different from each other. And the duration of stripes in frequency range are also various among them.

Each stripe of the low frequency part at high altitude comprised two different parts. Take the first stripe as an example, from 07:07:45.6 UT to 07:07:46.8 UT, the frequency drift rate is about 21.8 MHz/s; and from 07:07:46.8 UT to 07:07:48.8 UT, the frequency drift rate is about 6.8 MHz/s. The contour of it was shown in Fig. 4. There was a breakpoint between the two parts. This suggests that N1 may be caused by the interaction between the slowly growing flare loops and the fast downward reconnection out flows from the reconnection site at higher

Table 1
The parameters of the right part of N1

Stripes	Duration of strip (s)	DsF (MHz)	FD (MHz/s)
1	2.197	36	12.9
2	2.248	28	12.5
3	1.736	28	14.8
4	2.043	28	14.1
5	6.300	52	8.3
6	1.668	20	11.5
7	2.500	20	8
7	3.556	−16	−4.5
8	2.222	8	3.6
8	2.222	−8	−3.6
9	3.720	32	8.6
10	1.935	12	6.2
11	15.758	−52	−3.3

The total bandwidth of N1 is 92 MHz. DsF, the duration of stripes in frequency range, which is defined as the ending frequency minus the beginning frequency of each stripe. FD, frequency drift rate of each stripe. The sequence numbers of stripes are decided from up to bottom and from left to right in the Fig. 3(b) of N1.

altitude (Lin et al., 2006). And the breakpoint of the stripe happened when the flare loop interacted with the downward flows.

2.3. Analysis of the Z2 and Z3

There are several mechanisms for zebra and fiber structures, and one generally accepted theory is DPR (Kuijpers, 1975; Zhelezniakov and Zlotnik, 1975). The model can best describe the observations and the conditions in the corona. However, fine structure spectral observations reveal a number of new features that cannot be easily interpreted by DPR such as quasi-parallel striped with a wave-like drift. Chernov (1976, 1996) and Maltseva and Chernov (1989) proposed that their origin can be explained by the whistler model: the interaction of plasma waves with whistler: $l + w \rightarrow t$. The fibers are likely associated with ducted propagation of whistler from the depths of the corona along a trap, while the zebra structure is associated with non-ducted propagation, oblique to the magnetic field, mainly at the top of the trap (Chernov, 1990 and Chernov et al., 2005). Both of the models can easily explain the common features, for example FD (absolute value of frequency drift rate) and DF (frequency difference between two neighboring zebra lines). We have payed more attention on DFs in present work.

In the whistler mode, the frequency separation between the stripes in emission and the adjacent absorption (Δf_{ea}) is approximately equal to the whistler frequency $f_w \approx 0.1 f_B$ (f_B: the electron cyclotron frequency) (Chernov, 1990). Assume that the frequency difference between two zebra lines is approximately two times of Δf_{ea}, the magnetic field can then be estimated. The results were shown in Table 2. We set the frequency to be 1.200 GHz, which is the middle frequency at our observational band. Then in DPR model, the harmonic number will be obtained from Eq. (1). The harmonic number of Z2 and Z3 were approximately equal to 10 and 15. The density of the particle inside the coronal loop can be obtained by Eq. (1) as shown in Table 2.

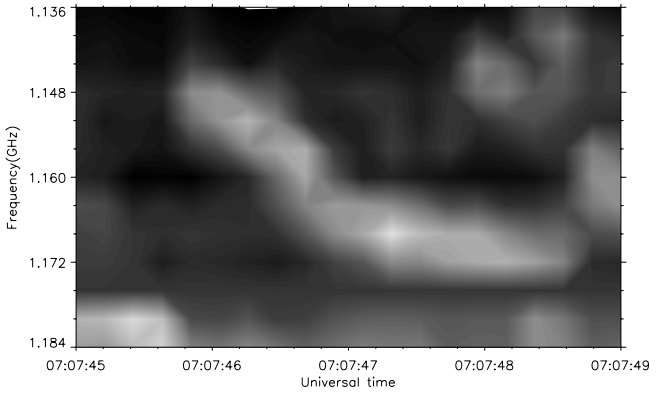

Fig. 4. The contour of the first stripe in right part of N1 from 07:07:45 UT to 07:07:49 UT. Two parts (fast frequency drifting and low frequency drifting) make up of the stripe, with a breakpoint between them.

Table 2
The parameters of Z2 and Z3

	DF (MHz)	B (G)	s	Density
$Z2$	24	42.9	9.9	1.76
$Z3$	16	28.6	14.99	1.77

DF, frequency difference between two neighboring zebra lines; B, the magnetic field value obtained by the whistler mode; s, the harmonic number of observed frequency in DPR model. The observed frequency was set to be 1.200 GHz. Density, the density of particles ($\times 10^{10}$ cm^{-3}).

3. Model of the coronal loop

To find the positions where the zebra patterns happened inside the loop, we need to specify a model for the magnetic field, the condition of plasma and the temperature in corona. The MDI observation provides the magnetic field of AR 10708 and RHESSI observation display the HXR emission at 4–6 keV, 6–8 keV, 12–25 keV, 25–50 keV bands. In the RHESSI images, the high energy panel show two foot points structure and EIT image shows loop structure. By comparison of the observations, we suppose a coronal loop model during the burst of the flare. Fig. 5 displays the model of coronal loop. The adopted magnetic field model is that of two dipoles with antiparallel magnetic fields, placed vertically bellow the photosphere. At the foot of the loop, the magnetic field is decided by MDI Data shown in Fig. 1. The distance between foot points is 2×10^9 cm which is obtained from the EIT image. At the top of the loop, the upper line is about 9×10^8 cm above the base of corona, and the lower line is about 7×10^8 cm above the base of corona as shown in Fig. 5.

As to the temperature, we have adopted a model with constant conductive flux in the region of temperature from

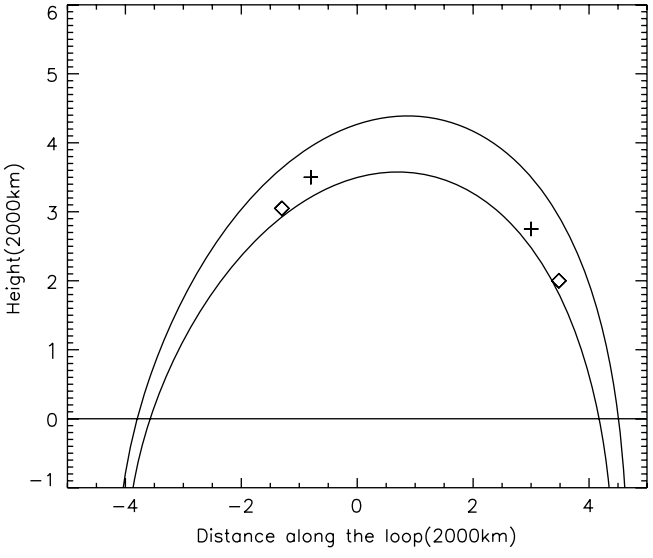

Fig. 5. The model of dipole magnetic field: the upper line of the loop is about 9×10^8 cm above the base of corona, the lower line is about 7×10^8 cm above the base of corona. The positions of Z2 and Z3 are marked by diamond (Z2) and plus (Z3) separately inside the loop.

10^5 K up to coronal temperature given by Eq. (2) (Alissandrakis et al., 1980).

$$T = \left[T_0^{7/2} + \frac{7}{2}\frac{F_c}{A}(z - z_0)\right]^{2/7}; T_0 < T < T_{cor} \quad (2)$$

Here F_c is the conductive flux, $F_c = 2 \times 10^6$ erg cm^{-2} s^{-1}, $A = 1.1 \times 10^{-6}$ cgs units, $T_0 = 10^5$ K, T_{cor} is the corona temperature, z_0 is the height at which $T = T_0$. The density model is based on the assumption of hydrostatic equilibrium for the gas pressure (Alissandrakis et al., 1980). For the temperature given by Eq. (2), the pressure is given by:

$$P = P_0 \exp(-8.9 \times 10^{-11}[T^{5/2} - T_0^{5/2}]/F_c) \quad (3)$$

where T_0 is the temperature at height z_0. Because the plasma beta value $\beta \ll 1$ and T in the result of our model are according with the conditions of the corona, we can calculate some parameters with the dipole model. Although the dipole model is too simple for the flare, the approximate parameters may be obtained to analyze the process of bursts. In Table 2, the magnetic field value in the whistler mode is presented when the stripe line occurred at 1.200 GHz. We calculated the magnetic field in our model and the positions when these fine structures happened are marked by diamond (Z2) and plus (Z3) separately in our coronal loop model. At 1.200 GHz, the positions of Z2 and Z3 are at the top of the flare loop which may correspond to the cusp area when magnetic reconnection occurred.

4. Discussion and conclusion

To summarize, the observations in the 1.100–1.340 GHz ranges by Solar Broadband Radio Dynamic Spectrometer (SBRS) in Huairou Station help us to learn the process about solar radio bursts, especially for the new fine structures. The observations of radio bursts at 07:00:00 UT–07:40:00 UT on December 1, 2004 exhibit a new pattern of fine structure. Three groups of fine structure bursts were found during the impulsive phase of the flare: N1, Z2, and Z3. Radio burst observations combined with HXR observations show that the HXR flux maintained at three subsequent plateaus when the three fine structures occurred. During each event, the HXR flux at both 12–25 keV band and 25–50 keV band had no obvious rise but plenty of oscillations. Obviously, Z2 and Z3 are classical zebra pattern. The total bandwidth of N1, duration of individual strip and frequency difference between two neighboring lines are different from those of Z2 and Z3. The value of frequency difference between two neighboring lines in N1 are also different from each other.

The first group of fine structures N1 has fast-and-slow frequency drift rate. The frequency drift rate of stripes at high altitude (low frequency) of N1 is faster than the stripes at lower altitude (high frequency). We suggest that the faster frequency drift part of the stripe is involved with the fast downward reconnection out flows from the reconnection site at higher altitude and the lower frequency drift part of stripe is due to the slow upward motion of flare loops (76 km/s) at lower altitude according to Eq. (4):

$$\upsilon \sim 2[\mathrm{d}f/\mathrm{d}t/f][n/(\mathrm{d}n/\mathrm{d}h)] = (\mathrm{d}f/\mathrm{d}t)/(\mathrm{d}f/\mathrm{d}h) \quad (4)$$

where υ is the velocity of flows, n is the density of the corona. The hight scale of the density is about 1.2×10^9 cm. As to each stripe at high altitude (low frequency band), there are two parts for the individual stripe. At the beginning of the stripe as shown in Fig. 4, the frequency drift rate is about 21.8 MHz/s. At about 07:07:46.8 UT, the frequency drift rate turned to be smaller than before, which is about 6.8 MHz/s. The faster frequency drift part of this stripe (21.8 MHz/s) shows that the velocity of the fast downward reconnection out flows from the reconnection site is about 438 km/s. And the slow motion of flare loop (76 km/s) may decelerate the fast flows, and the frequency drift rate is decreased to be 6.8 MHz/s. These results are agreeable with theoretical analysis of Lin (2004) that the rising speed of the low part of the current sheet is from several tens km/s to a maximum speed of ~120 km/s in a few minutes.

We adopted DPR model and whistler model at the same time to analyze the zebra pattern structures. We assume that the two groups of zebra structures were produced at different part of the flare loop. Fig. 5 showed the flare loop and the position of Z2 and Z3 when they occurred. We recorded the time of peak flux at 1.200 GHz of each events: 07:08:00 UT, 07:09:05 UT, 07:11:00 UT. The time interval between Z2 and Z3 is: $t_{2,3} = 115$ s. In the left part of the loop, the distance between neighboring fine structures were: $D_{2,3} = 18$ Mm. In the right part of loop, $D'_{2,3} = 17$ Mm. Then the variation rate of the zebra sources Z2 and Z3 are $v_{2,3} = 157$ km/s of the left part of loop and $v'_{2,3} = 148$ km/s of the right part of loop. The two zebras are both located on the loop top in our flare loop model, they may reflect the conditions of cusp region during the flare. We consider that 157 km/s and 148 km/s may indicate the variation rate of the zebra sources Z2 and Z3. Therefore it may correspond to the rising speed of the low part cusp region where zebra patterns occurred. Although our field calculation is based on a static model but the results are agreeable with the frequency drift results as mentioned above.

Further studies are needed to analyze the origin of N1 structures by comparison with other space- and ground-based observations, which is under investigation separately.

Acknowledgments

The authors thank RHESSI and EIT teams for providing data. The MDI data were obtained from the MDI database. This work was supported by MOST (2006CB806301) and NSFC (10225313, 1033303) Grants. Dr. Jun Lin and G.P. Chernov are acknowledged for helpful discussions.

References

Alissandrakis, C.E., Kundu, M.R., Lantos, P. A model for sunspot associated emission at 6 CM wavelength. Astron. Astrophys. 82, 30, 1980.

Aschwanden, M. Physics of the Solar Corona. Praxis Publication, Chichester, UK, 2004.

Bastian, T.S., Benz, A.O., Gary, D.E. Radio emission from solar flares. Annu. Rev. Astron. Astrophys. 36, 131, 1998.

Chernov, G.P. Microstructure in continuous emission of type IV meter bursts. Modulation of continuous emission by wave packets of whistlers. Soviet Astron. 20, 582, 1976.

Chernov, G.P. Whistlers in the solar corona and their relevance to fine structures of type IV radio emission. Solar Phys. 130, 75, 1990.

Chernov, G.P. A manifestation of quasilinear diffusion in whistlers in the fine structure of type IV solar radio bursts. Astronomy Rep. 40, 561, 1996.

Chernov, G.P., Fu, Q.J., Lao, D.B., Hanaoka, Y. Ion-sound model of microwave spikes with fast shocks in the reconnection region. Solar Phys. 201, 153, 2001.

Chernov, G.P., Yan, Y.H., Fu, Q.J., Tan, Ch.M. Recent data on zebra patterns. Astron. Astrophys. 437, 1047, 2005.

Delaboudiniere, J.-P., Artzner, G.E., Brunaud, J., Gabriel, A.H., Hochedez, J.F., Millier, F., Song, X.Y., Au, B., Dere, K.P., Howard, R.A., Kreplin, R., Michels, D.J., Moses, J.D., Defise, J.M., Jamar, C., Rochus, P., Chauvineau, J.P., Marioge, J.P., Catura, R.C., Lemen, J.R., Shing, L., Stern, R.A., Gurman, J.B., Neupert, W.M., Maucherat, A., Clette, F., Cugnon, P., van Dessel, E.L. EIT: Extreme-ultraviolet imaging telescope for the SOHO mission. Solar Phys. 162, 291, 1995.

Fu, Q.J., Ji, H.R., Qin, Z.H., Xu, Zh.C., Xia, Zh.G., Wu, H.A., Liu, Y.Y., Yan, Y.H., Huang, G.L., Chen, Zh.J., Jin, Zh.Y., Yao, Q.J., Cheng, C.L., Xu, F.Y., Wang, M., Pei, L.B., Chen, Sh.H., Yang, G., Tan, Ch.M., Shi, S.B. A new solar broadband radio spectrometer (SBRS) in China. Solar Phys. 222, 167, 2004.

Ji, H.R., Fu, Q.J., Yan, Y.H., Liu, Y.Y., Chen, Zh.J., Tan, Ch.M., Cheng, C.L., Lao, D.B., Li, Sh.K., Wang, Zh.Q., Yu, M.H., Liu, J.N., Zhang, L.K., Gao, J.Y. A new solar radio spectrometer at 1.10C2.06 GHz and first observational results. Chin. J. Astron. Astrophys. 3, 433, 2005.

Kuijpers, J. Generation of intermediate drift bursts in solar type IV radio continua through coupling of whistlers and Langmuir waves. Solar Phys. 44, 173, 1975.

Kruger, A.. Introduction to Solar Radio Astronomy and Radio Physics. Reidel, Dordrecht, 1979.

LaBelle, J., Treumann, R.A., Yoon, P.H., Karlicky, M. A model of zebra emission in solar type IV radio bursts. Astrophys. J. 593, 1195, 2003.

Ledenev, V.G., Yan, Y., Fu, Q. Interference mechanism of ''Zebra-Pattern'' formation in solar radio emission. Solar Phys. 233, 129, 2006.

Lin, J. Motions of flare ribbons and loops in various magnetic configurations. Solar Phys. 222, 115, 2004.

Lin, J., Mancuso, S., Vourlidas, A. Theoretical investigation of the onsets type II radio bursts during solar eruptions. Astrophys. J. 649, 1110, 2006.

Lin, R.P., Dennis, B.R., Hurford, G.J., Smith, D.M., Zehnder, A., Harvey, P.R., Curtis, D.W., Pankow, D. The Reuven Ramaty high-energy solar spectroscopic imager (RHESSI). Solar Phys. 210, 3, 2002.

Liu, Y.Y., Fu, Q.J., Yan, Y.H., Tan, Ch.M. New result obtained from the solar radio spectrometer in decemeter wavelength with super-high temporal resolution. Publ. Nat. Astron. Obs. China 3, 119, 2006.

Maltseva, O.A., Chernov, G.P. Whistler ray tracing calculations in the solar corona. Kinematika i Fizika Nebesnykh Tel. 5, 39, 1989.

Scherrer, P.H., Bogart, R.S., Bush, R.I., Hoeksema, J.T., Kosovichev, A.G., Schou, J., Rosenberg, W., Springer, L., Tarbell, T.D., Title, A., Wolfson, C.J., Zayer, I. MDI engineering team, the solar oscillations investigation—Michelson doppler imager. Solar Phys. 162, 129, 1995.

Slottje, C. Atlas of fine structure of dynamic spectra of solar type IV-dm and some type II radio bursts, 1981.

Zhelezniakov, V.V., Zlotnik, E.Ia. Cyclotron wave instability in the corona and origin of solar radio emission with fine structure. I—Bernstein modes and plasma waves in a hybrid band. Solar Phys. 44, 461, 1975.